Sensors & Actuators: B. Chemical 348 (2021) 130716

Contents lists available at ScienceDirect

Sensors and Actuators: B. Chemical

journal homepage: www.elsevier.com/locate/snb

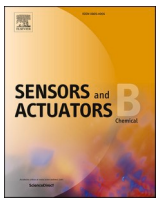

Sensing performance of Pd nanogap supported on an elastomeric substrate in a wide temperature range of –40 to 70 °C

Seyoung Park [a], Soo-Min Lee [a], Jin-Kyo Jeong [b], Donggu Kim [c], Hyunsoo Kim [c], Hyun-Sook Lee [a,*], Wooyoung Lee [a,*]

[a] Department of Materials Science and Engineering, Yonsei University, 50 Yonsei-ro, Seodaemun-gu, Seoul 03722, Republic of Korea
[b] Department of Vehicle Convergence Engineering, Yonsei University, 50 Yonsei-ro, Seodaemun-gu, Seoul, 03722, Republic of Korea
[c] Electronic device research team, Hyundai Kia Automotive Group, 37 Cheoldobangmulgwan-ro, Uiwang-si, Gyeonggi-do, 437-815, Republic of Korea

ARTICLE INFO

Keywords:
Hydrogen sensors
Pd nanogap
Polydimethylsiloxane (PDMS)
Elastomeric substrate
Subzero operating temperature
Safety sensor

ABSTRACT

We examined the effect of environmental temperature (–40 to 70 °C) on the hydrogen sensing performance of a Pd nanogap sensor supported on an elastomeric polydimethylsiloxane (PDMS) substrate. Sensing tests were conducted using various sensors with different gap widths, prepared with different tensile strains. All sensors operated in an "On-Off" mode with a rapid response time of ~1 s at the operating temperatures. The sensing performance was significantly influenced by the high thermal contraction/expansion properties of the PDMS substrate, depending on the environmental temperature. At subzero temperatures (0, –20, and –40 °C), the sensing performance was improved owing to the gap narrowing. At high temperatures (above 40 °C), it decreased owing to the gap broadening. The detection limit was 300 ppm at subzero temperatures but >1% at high temperatures. The results reveal that the Pd nanogap sensor on PDMS is more suitable for detecting H_2 at subzero temperatures. In addition, the sensor showed excellent reproducibility for hundreds of sensing cycles at 25 °C and –40 °C. Furthermore, the sensor was stable to high humidity (above 70 RH%) at 25 °C. Our study demonstrated that the Pd nanogap sensor on a PDMS substrate is a possible candidate for use as an on-board safety H_2 sensor in hydrogen-electric vehicles.

1. Introduction

Recently, the hydrogen economy has gained increasing attention globally. In particular, the use of hydrogen-electric vehicles is expected to increase in major countries, such as the United States, Germany, China, and Japan, which are the largest global automobile markets expanding the demand for automotive hydrogen sensors. The global automotive hydrogen sensor market is expected to reach USD 17.6 million in 2027 [1]. To avoid the explosion risk of highly flammable H_2, it is essential to develop a sensor that can detect H_2 leaks sensitively and rapidly. The Department of Energy (DOE) in the United States has provided target specifications for H_2 safety sensors for various applications [2,3]. In particular, it has been reported that on-board safety H_2 sensors in fuel cell vehicles should be operational in the temperature range of –40 to 40 ℃ and a relative humidity range of 5–95% [2,3]. The sensor must also meet other requirements, such as an H_2 detection limit of 0.1%, a response time of less than 1 s for 1% H_2, and a desired lifetime of 10 years [2,3].

Various types (catalytic, thermal conductivity, electrochemical, resistance-based, work function-based, and optical) of H_2 sensors operating with different sensing mechanisms have been developed and commercially available to date [4]. However, most sensors have an H_2 detection limit greater than 1% and a response time longer than 10 s [4]. The selective detection of H_2 is low, power consumption is high, and sensor fabrication is complicated [4]. Moreover, the lowest operating temperature is –20 ℃, which is much higher than the DOE requirement. As a result, existing H_2 sensors do not yet meet all the stringent criteria, and more research is needed to develop sensors that satisfy the target specifications.

Sensing materials are essential for achieving high sensitivity and selectivity. In particular, Pd-based materials have been used extensively for H_2 sensors because they provide high sensitivity and selectivity owing to the high affinity of Pd for H_2. To achieve high sensitivity and low power consumption, one-dimensional Pd-including nanowires [5,6] and nanotubes [7] have been investigated. In addition, Pd nanoparticles have been functionalized on carbon nanotubes [8,9] and

* Corresponding authors.
E-mail addresses: h-slee@yonsei.ac.kr (H.-S. Lee), wooyoung@yonsei.ac.kr (W. Lee).

https://doi.org/10.1016/j.snb.2021.130716
Received 18 June 2021; Received in revised form 16 August 2021; Accepted 2 September 2021
Available online 7 September 2021

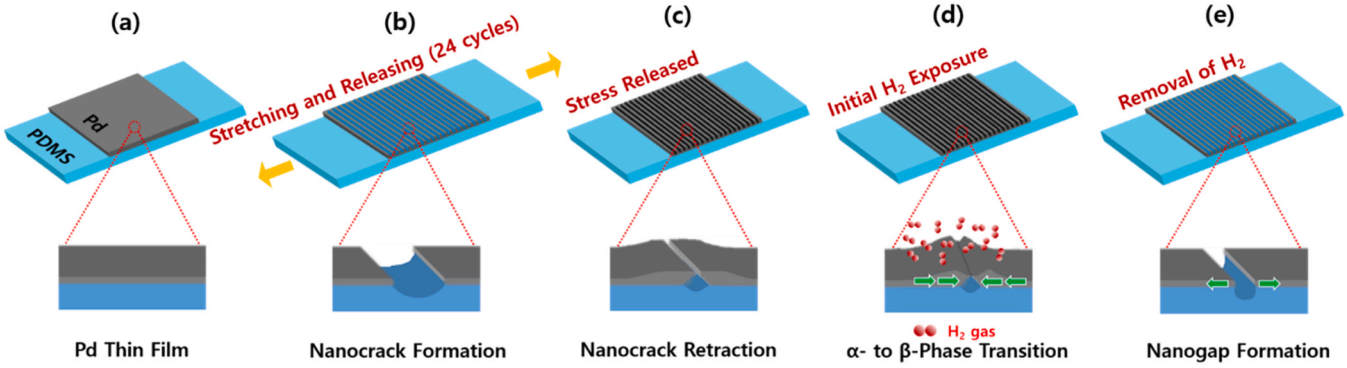

Fig. 1. Schematic of the process of fabrication of nanogaps in a Pd thin film on an elastomeric PDMS substrate by mechanical stretching/compression.

semiconducting nanowires (such as InAs [10] and Si [11,12]). In particular, many studies have investigated various metal oxide semiconductors (such as ZnO [13], NiO [14], TiO_2 [15], In_2O_3 [16], SnO_2 [17], and WO_3 [18]) decorated with Pd nanoparticles [19].

Among the various types of Pd-based H_2 sensors, Pd nanogap-based sensors were first introduced using Pd mesowires comprising Pd nanoparticles [5] to improve the rapid response and short recovery time by applying an "On-Off" sensing mechanism. Subsequently, to improve the sensitivity of Pd mesowires, various electrodeposition methods have been proposed using different lithographic patterning [20,21] and different templates [22,23]. Among the various types of Pd nanogap-based H_2 sensors, the Pd nanogap sensor supported on a poly (dimethylsiloxane) (PDMS) substrate has provided significant advances in H_2 sensing properties, such as high sensitivity, selectivity, and rapid response and recovery times [24,25]. The Pd nanogaps were easily formed on PDMS by simply performing mechanical stretching/compression cycles. H_2 sensing of the Pd nanogap sensors occurs by an "On-Off" mechanism at room temperature. When exposed to H_2, the Pd nanogap sensor is in an "On" state (closed nanogap) because of the volume expansion of Pd by absorbing H atoms. In contrast, upon removing H_2, the sensor is in an "Off" state (open nanogap) because of the volume contraction of Pd by desorbing H atoms. This new approach was achieved using the elastic property of PDMS without lithography, which is very cost-effective. The Pd nanogap sensor on PDMS can detect a lower limit of 0.05% H_2, has a fast response time of 0.67 s for 2% H_2, and can operate at room temperature [24,25].

Since the first report on this sensor [24], there have been many studies, describing reduced detection limits, enhanced sensitivity and selectivity, and improved stability against moisture interference [26–34]. However, all these studies were conducted at room temperature. PDMS has a high coefficient of thermal expansion (3.4×10^{-4} °C^{-1} [35]) compared to other flexible polymers [36,37]. Moreover, the PDMS silicone elastomer retains its flexibility over a temperature range of –45 to 200 °C for an extended time [35]. Thus, using the high coefficient of thermal expansion of PDMS, it is possible to control the Pd nanogap width on the PDMS substrate by controlling the environmental temperature.

In this study, we investigated the effect of environmental temperature on the sensing performances of the Pd nanogap sensors with different gap widths on the PDMS substrate. The width of the Pd nanogap was controlled by applying various tensile strains. The hydrogen sensing tests were performed in a wide range of environmental temperatures ranging from –40 to 80 ℃, which is the temperature range specified by the DOE [2,3]. The detection limits and response times were investigated under extreme temperature conditions. We also tested the reproducibility for hundreds of sensing cycles and the sensing stability of the moisture effect for various relative humidities.

2. Materials and methods

2.1. Fabrication of Pd nanogaps on elastomeric PDMS substrate

The elastomeric substrates were prepared using cured PDMS. A silicone elastomer (Sylgard 184, Dow Corning Corp.) of the base material was mixed with a curing agent at an optimized weight ratio of 10:1. The PDMS mixture was kept in a vacuum desiccator at room temperature for 20 min to remove air bubbles and then cured at 75 °C for 4 h on a hot plate. The cured PDMS was cut into pieces with an area of 16×10 mm^2 and a thickness of 1 mm for use as a substrate. A thin Pd film (10 nm, size $= 10 \times 10$ mm^2) was fabricated on the surface of the PDMS substrate (Fig. 1(a)) using an ultrahigh vacuum direct current (DC) magnetron sputtering system. The base pressure of the DC sputtering chamber was 7.0×10^{-8} Torr. Pd deposition was conducted at a working pressure of 1.2×10^{-4} Torr under 34 sccm of Ar gas flow using a high-purity Pd target (99.99%). The Pd deposition rate was approximately 3.3 Å/s at an applied power of 20 W.

To make Pd nanocracks on the PDMS substrate, tensile strain was uniformly applied to the specimen of the Pd film/PDMS layers using a micro tensile tester (Linkam Scientific Instruments, TST350). Various nanocracked samples were prepared using different tensile strains of 25%, 50%, 75%, and 100% with a constant tensile velocity of 500 μm/s. The tensile strain value was defined as $[(l-l_0)/l_0 \times 100]$%, where l_0 and l are the initial and final lengths before and after the tensile stress is applied, respectively. The nanocracks were produced during the 24 stretching/releasing cycles at room temperature (Fig. 1(b)). After the stress was released, the nanocracks were retracted and connected to each other (Fig. 1(c)).

To generate Pd nanogaps from the closed nanocracks, the sample was subjected to one cycle of exposure and removal of H_2 gas. When the sample is exposed to H_2, the ends of the broken Pd nanocracks are connected, owing to the volume expansion of Pd because the dissociated H atoms from H_2 molecules are absorbed into the interatomic sites of Pd (α- to β-phase transition [38,39]) (Fig. 1(d)). When H_2 gas is removed, the absorbed hydrogen atoms are rapidly desorbed, resulting in the conversion of PdH_x to Pd (β- to α-phase transition [38,39]), and the Pd ends are relocated relative to the PDMS cracks (Fig. 1(e)). Finally, opened Pd nanogaps are formed on the PDMS substrate. For one cycle of initial exposure, 2% H_2 in N_2 was used.

2.2. Characterization of Pd nanogaps

The distribution of nanogaps on the PDMS substrate, spacing between adjacent nanogaps, and width of nanogaps for the various specimens prepared using different strains were analyzed using optical microscopy (OM, Olympus BX41 M) and scanning electron microscopy (SEM, JEOL JSM-6701F).

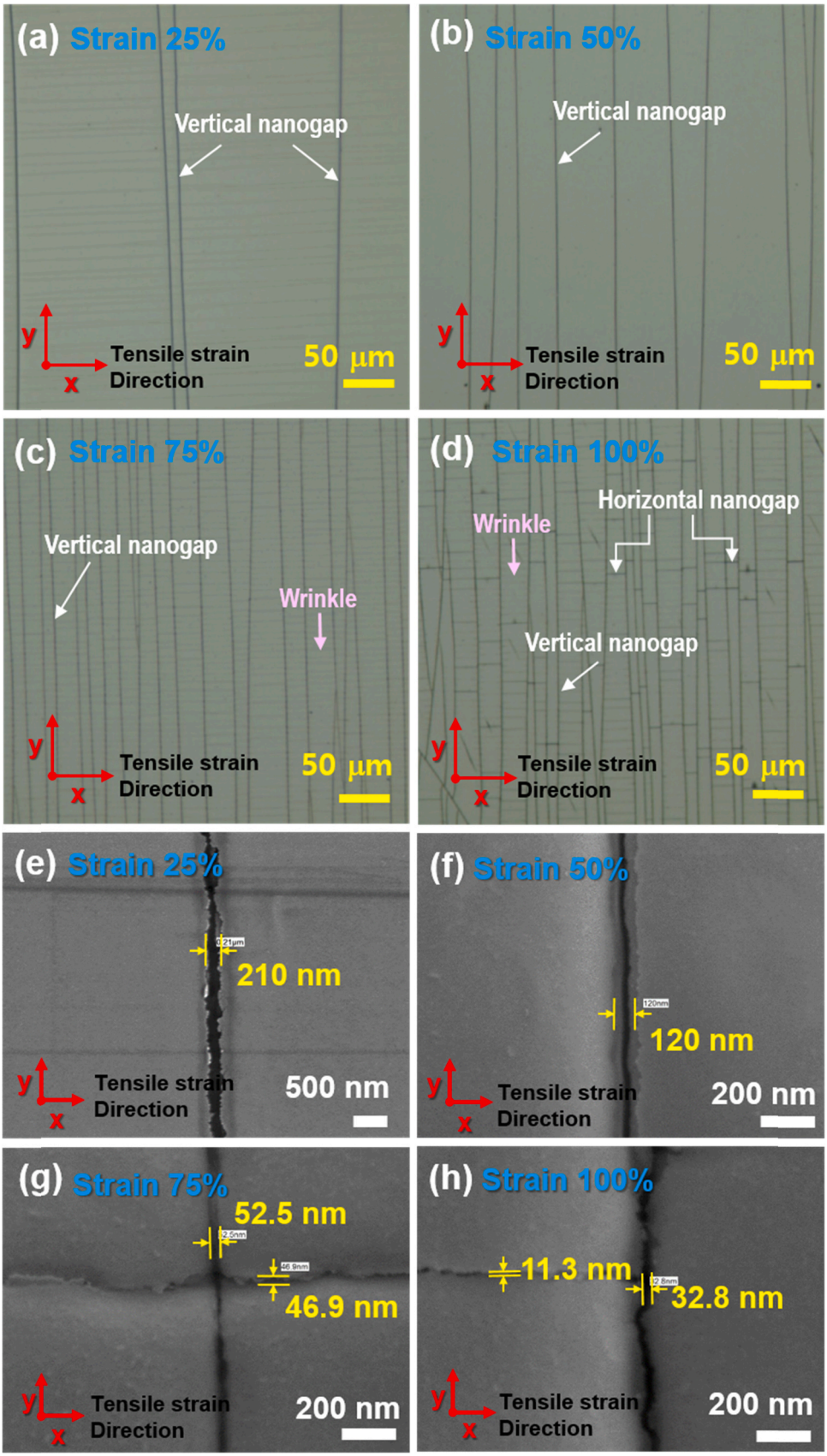

Fig. 2. Top-view optical microscopy; (a)–(d) and scanning electron microscopy; (e)–(h) images of nanogaps formed in a Pd thin film on a PDMS substrate by applying tensile strains of 25%, 50%, 75%, and 100%.

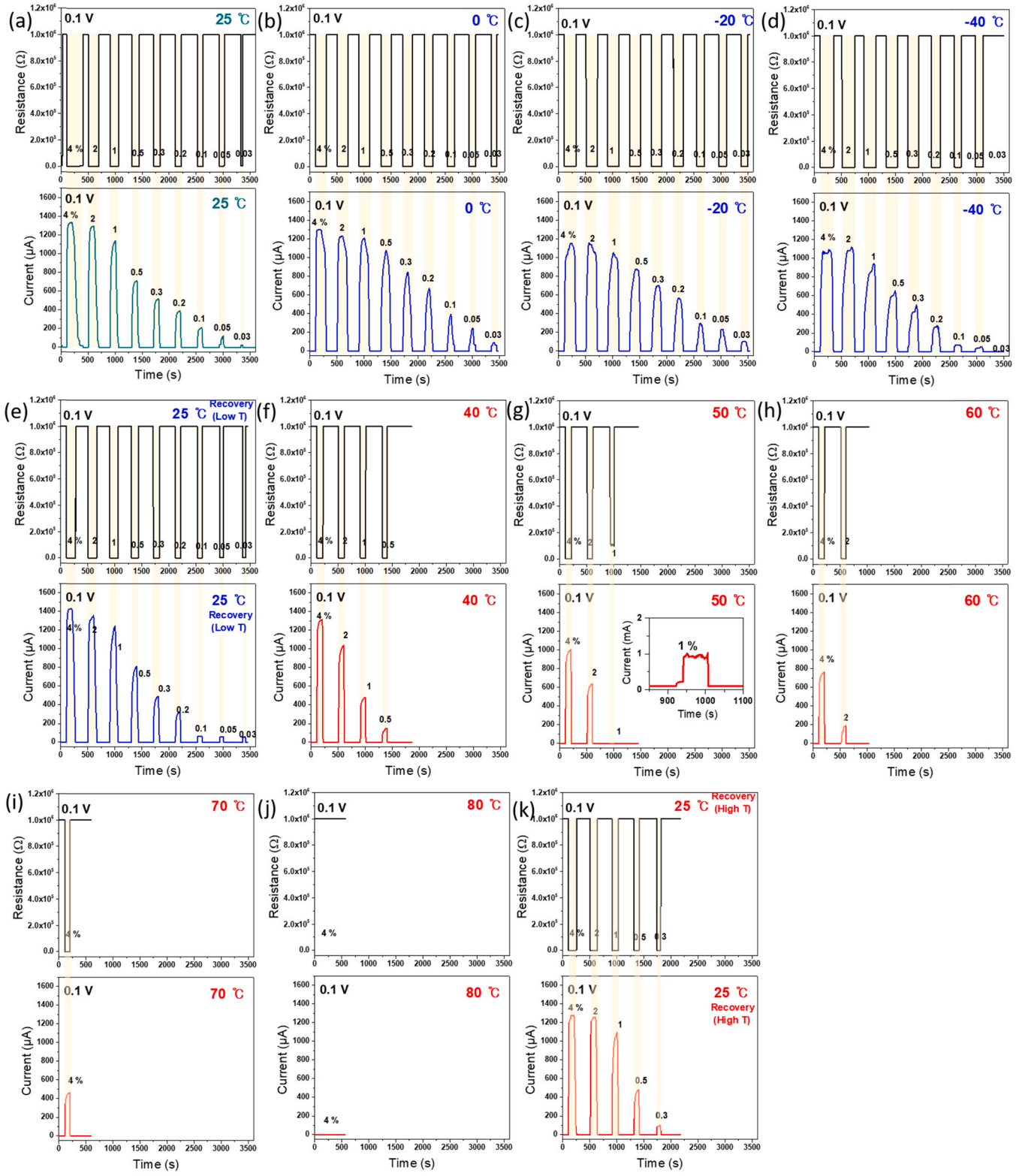

Fig. 3. Real-time electrical responses—resistance (top) and current (bottom)—of the sensor prepared with 75% tensile strain to a gradually decreasing H_2 concentration from 4% to 0.03% at a wide range of operating temperatures from –40 to 80 ℃. Electrical currents were measured in the following temperature sequence: (a) 25 ℃, (b) 0 ℃, (c) –20 ℃, (d) –40 ℃, (e) 25 ℃, (f) 40 ℃, (g) 50 ℃, (h) 60 ℃, (i) 70 ℃, (j) 80 ℃, and (k) 25 ℃.

2.3. Hydrogen sensing measurements

The hydrogen sensing measurements of the as-prepared Pd nanogap sensors fabricated on the PDMS elastomeric substrate were carried out using a microprobe station system (Nextron MPS-PT) equipped with a source–measure unit (Keithley 6220 and Keithley 2182). A constant voltage of 0.1 V was applied with a time interval of 1 s. The inner volume of the sealed gas chamber was approximately 100 cm^3. The chamber had a gas inlet and an outlet. The concentration of H_2 was controlled by mixing a high-concentration H_2 (4%, >99.999%) with N_2

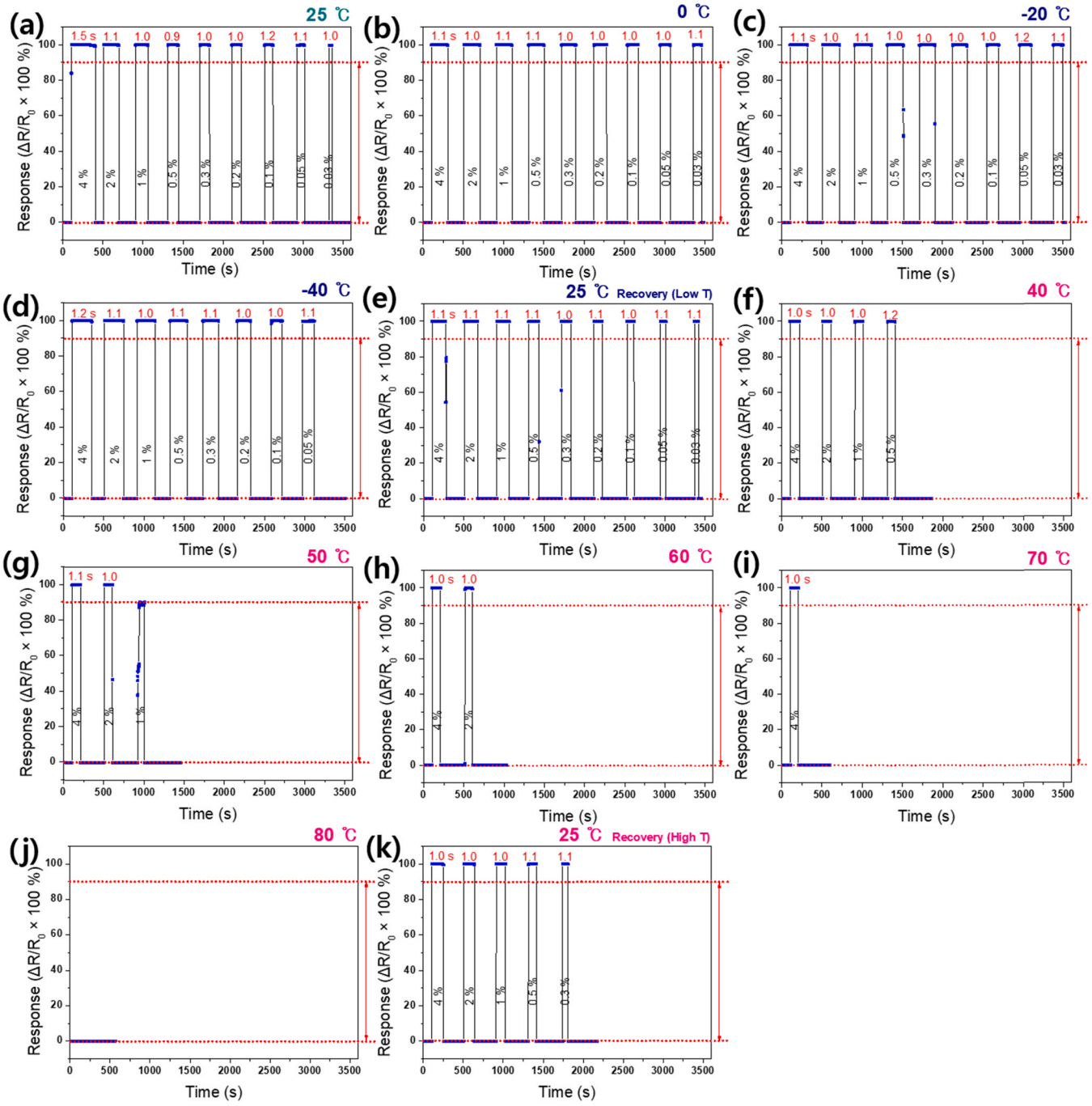

Fig. 4. Response versus time curve for the sensor prepared with 75% tensile strain. The response was converted from the electrical resistance responses. The response time was calculated using a definition of the time to reach 90% of the total change of resistance. The average response times are approximately 1 s for 0.03–4% H_2 at a wide range of low and high temperatures. The time interval between data points is 1 s.

(>99.999%) gas using mass flow controllers (MFCs). Owing to safety concerns, we used N_2 as a carrier gas to control the H_2 concentration under conditions identical to those of the 4% H_2 gas cylinder. H_2 gas mixed with the desired concentration was fed into the gas chamber through the inlet.

To obtain the electrical measurements corresponding to the H_2 sensing properties, a tungsten tip was placed on two electrodes fabricated using silver paste on the surface of a Pd film consisting of a nanogap. The working temperature of the sensor was controlled in the range of –40 to 80 ℃ by adjusting the temperature of the sample stage in the chamber. The sample stage (18 mm × 18 mm) made of aluminum nitride was cooled and heated using the Peltier effect. The temperature was measured using a Pt sensor mounted on the micro probe station.

3. Results and discussion

The distribution of Pd nanogaps on the PDMS substrates formed with different strains was observed using OM. Fig. 2(a)–(d) presents the top-view of the OM images. Twenty-four cycles of tensile strain were applied in the *x*-direction with strains of 25%, 50%, 75%, and 100% under a constant tensile velocity of 500 μm/s. In all strains, vertical nanogaps were produced along the direction of tensile strain. With increasing tensile strain, the spacing between adjacent nanogaps became narrow: ~145 μm for 25%, 30–85 μm for 50%, 10–40 μm for 75%, and

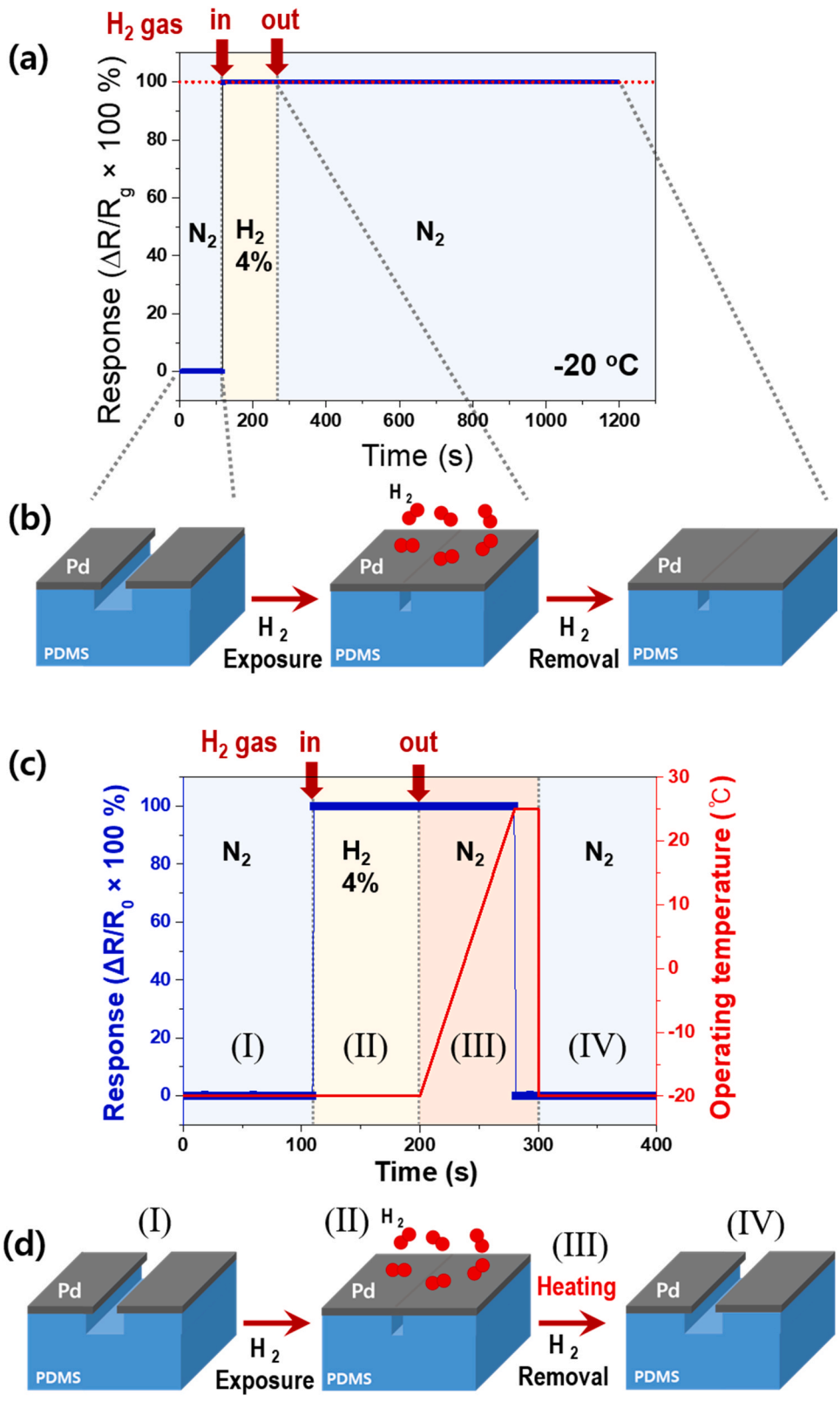

Fig. 5. (a) Response versus time curve of the 75%-strained sensor exposed to 4% H_2 at the subzero operating temperature of –20 ℃ and (b) illustrations of the nanogap close–open operation of the sensor corresponding to the electrical responses shown in (a); (c) Response versus time curve of the 75%-strained sensor exposed to 4% H_2 at–20 ℃. The heating procedure was added when the H_2 gas is removed to open the nanogap. (d) illustrations of the nanogap close–open operation of the sensor corresponding to the electrical responses shown in (c).

10–25 μm for 100%. In addition, at strains of 75% and 100%, horizontal nanogaps were created along the *y*-direction. Therefore, the density of the formed nanogaps increased with increasing tensile strain.

The average width of the nanogaps formed with different tensile strains was analyzed using SEM. Fig. 2(e)–(h) show representative SEM images of the nanogaps distributed in the specimens; the gap width is reduced with an increase in strain. The average width of the vertical nanogap was approximately 210 nm for the 25% strain and 120 nm for the 50% strain. The vertical and horizontal nanogaps have widths of ~52 nm and ~47 nm for 75% strain, respectively, and ~33 nm and ~11 nm at 100% strain, respectively. As shown in Figs. 2 and 3, with an increase in the tensile strain, the gap width decreases and more

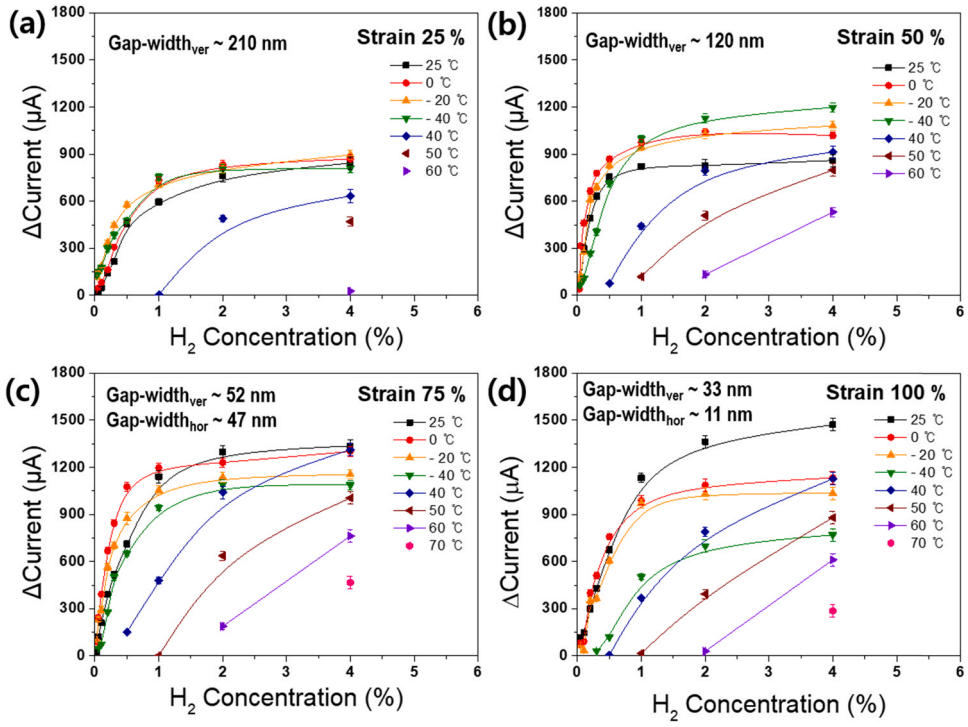

Fig. 6. Current variation versus H_2 concentration curves for various sensors prepared with different tensile strains of (a) 25%, (b) 50%, (c) 75%, and (d) 100% in response to 0.03–4% H_2 at different operating temperatures (–40 to 70 ℃). Representative gap widths of vertical and horizontal nanogaps formed in the sensor with different tensile strains are presented in the inset.

nanogaps are formed; this finding is consistent with our previous work [32].

The Hydrogen sensing abilities of the Pd nanogaps on PDMS substrates were examined over a wide range of operating temperatures from –40 to 80 ℃. The operating temperature of the sensor was set in two steps: (i) 25 ℃ → –40 ℃ → 25 ℃ and (ii) 25 ℃ → 80 ℃ → 25 ℃. Real-time electrical responses were measured for various sensors prepared with different tensile strains (25%, 50%, 75%, and 100%). Representative variations of resistance (top) and current (bottom) in real-time under exposure to gradually decreased H_2 concentrations from 4% to 0.03% were presented for the sensor prepared with 75% strain, as shown in Fig. 3. The current variations for the 25%, 50%, and 100% strains are presented in Figs. S1, S3, and S5, respectively, in the Supplementary Material. The on-board safety sensor must be able to detect hydrogen gas at concentrations as low as 0.1–10% [2,3]. In a previous study, the current change in the Pd nanogap sensor on the PDMS substrate indicated the same saturation value for H_2 concentration, from 4% to 10% [24]. Therefore, in this study, we investigated the sensing performance for H_2 concentrations of up to 4%. The results show that the sensor operates in an "On-Off" mode at all the tested temperatures (–40 to 70 ℃). The current flow (a significant decrease in resistance) appears when hydrogen is exposed. This is because the nanogaps are closed due to the volumetric expansion of Pd, resulting from hydrogen absorption into the Pd lattice. The maximum width of a nanogap that can be closed via H_2 absorption can be estimated by multiplying the average inter-crack distance and the ratio of lattice expansion [29]. For example, the 75%-strained sensor has an average inter-crack distance of 18 μm; thus, nanogaps up to 630 nm in width can be closed at room temperature assuming 3.5% lattice expansion, which is the lower boundary of the β PdH_x phase [38,39]. Therefore, the 75%-strained sensor can detect a low H_2 concentration of 300 ppm because the actual width of the nanogap was approximately 50 nm, as shown in Fig. 2(g). Furthermore, the sensor operates in an "On-Off" mode and can detect a low H_2 concentration of 300 ppm at subzero temperatures (0, –20, and –40 ℃), as shown in Fig. 3(b)–(d). The detection limit of 300 ppm sufficiently satisfies the DOE specifications (0.1% H_2) [2,3] even at an extremely low temperature of –40 ℃. However, as the operating temperature increased above 40 ℃, the current response decreased, and the detectable H_2 concentration increased. The H_2 detection limits were 0.5% at 40 ℃ and 4% at 70 ℃. When the operating temperature was increased to 80 ℃, the sensor no longer exhibited a sensing response (Fig. 3(j)). After cooling to 25 ℃, it showed a normal "On-Off" sensing reaction on exposure to H2 (Fig. 3(k)).

The response times of the sensor for the detection of H_2 at various low and high operating temperatures were evaluated from the response curves. The response in time was obtained from the general definition of the resistance change relative to the initial resistance ($|R - R_0|/R_0 \times 100$). Fig. 4 shows the real-time response of the 75%-strained sensor. Those for the 25%, 50%, and 100% strains are presented in Figs. S2, S4, and S6, respectively, in the Supplementary material. As shown in Fig. 4, the response reached 100% for all the H_2 concentrations at the operating temperatures. This is because the sensor operates in an "On-Off" mode. The response time, defined as the time required to reach 90% of the total change in response, was calculated and is presented in Fig. 4. The average response time of the 75%-strained sensor was approximately 1 s for all H_2 concentrations at the operating temperatures. Therefore, the Pd nanogap sensor on the PDMS elastomeric substrate is suitable for detecting leaked hydrogen within a faster time of 1 s, meeting the specifications set by the DOE.

At subzero temperatures (0, –20, and –40 ℃), the sensor did not return to the initial open-gap state even after H_2 removal. Fig. 5(a) shows the real-time response for exposure to 4% H_2 at –20 ℃. A response of 100%, indicating the flow of the saturation current, was observed even after removing the hydrogen gas. This implies that the closed nanogaps during H_2 exposure do not open at –20 ℃ even after removing H_2 gas, as illustrated in Fig. 5(b). This can be attributed to the contraction and freezing of the PDMS substrate at the subzero temperature, owing to its high thermal expansion coefficient (3.4×10^{-4} ℃$^{-1}$). Therefore, to recover the sensor to the initial open-gap state (stage I in Fig. 5(d)), a heating process had to be included. The resultant response

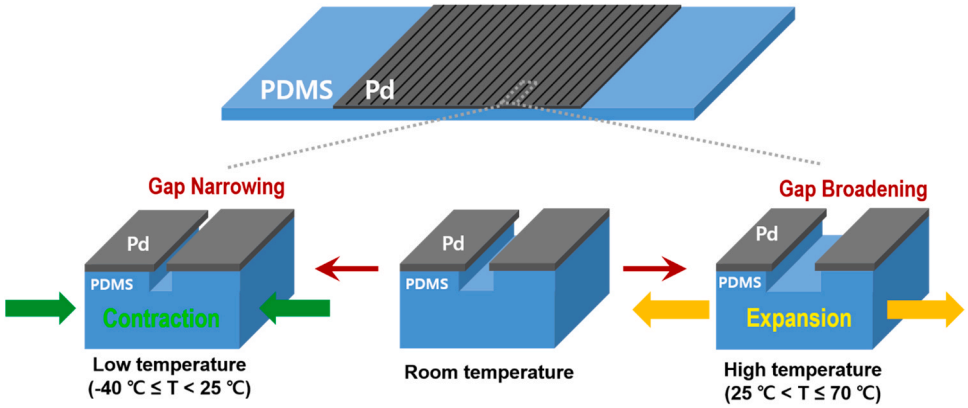

Fig. 7. Schematics of the sensing mechanism for the effect of low and high environmental temperatures on the sensing performance of the Pd nanogap sensor on an elastomeric PDMS substrate.

curve is displayed along with the temperature profile in Fig. 5(c). The sensor in the closed-gap state after H_2 exposure at –20 ℃ (stage II in Fig. 5(d)) was heated to a temperature of 25 ℃ with H_2 removal (stage III in Fig. 5(d)) to make the open-gap stage by thermal expansion of PDMS. Subsequently, the operating temperature was cooled back to –20 ℃ to measure the current response to the next H_2 concentration, and the nanogap remained in the open state, as illustrated in stage III in Fig. 5(d).

To optimize the tensile strain values to fabricate the best sensor that can operate with good sensing ability at various environmental temperatures, the current change, implying the sensing response, was compared in the sensors prepared with different strains (25%, 50%, 75%, and 100%). The current change measured at different operating temperatures (–40 to 70 ℃) with decreasing H_2 concentrations is summarized in Fig. 6. At 25 ℃, the highest current change is shown in the sensor with 100% strain, owing to the higher density of the nanogap and the smallest gap width (~33 nm for the vertical gap and ~11 nm for the horizontal gap). However, in the subzero temperature range (0, –20, and –40 ℃), the sensing performance of the 100%-strained sensor was significantly reduced, as shown in Fig. 6(d). However, the sensing degradation of the 75%-strained sensor at low temperature was smaller than that of the 100%-strained sensor (Fig. 6(c)). In particular, for the 50%-strained sensor, the sensing performance at subzero temperatures was improved compared to that at 25 ℃ (Fig. 6(b)). For the 25%-strained sensor, the sensing performance is unchanged over a wide range from room temperature (25 ℃) to subzero temperature (–40 ℃).

The results in Fig. 6 reveal that the sensing performances at subzero temperatures are strongly affected by the variation in the gap widths of Pd on PDMS with decreasing temperature. As illustrated in Fig. 7, the elastomeric PDMS substrate can shrink at subzero temperatures, and thus the Pd nanogaps may become narrower. The significant sensing degradation at 100% strain can be explained by the fact that the gap smaller than ~40 nm is closed owing to the PDMS contraction at the subzero temperature before H_2 exposure, and the remaining broader

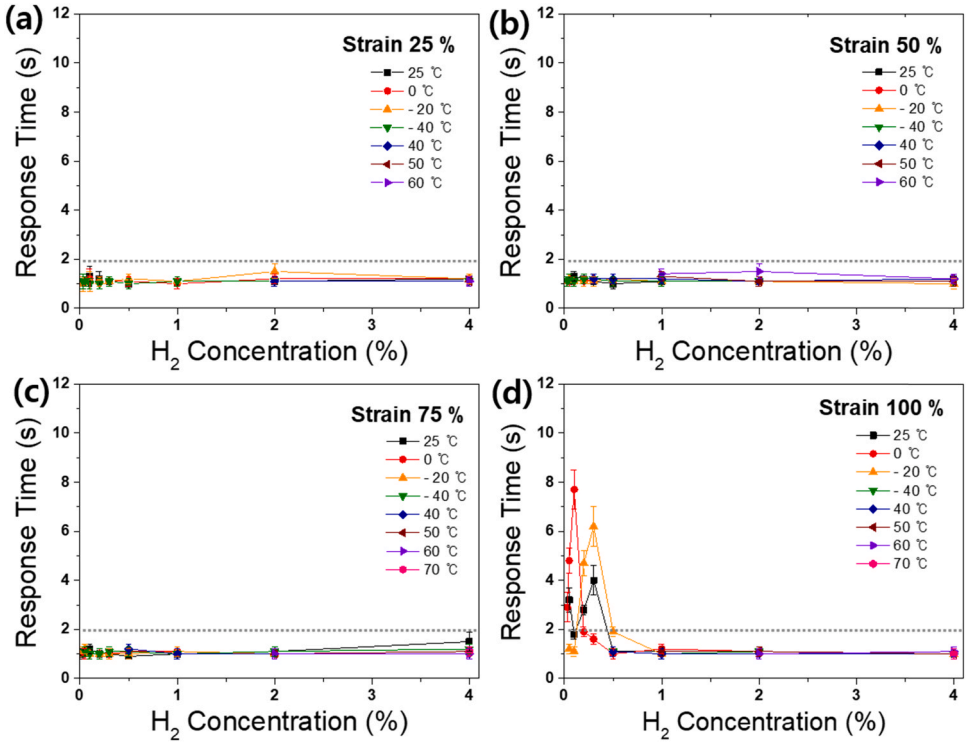

Fig. 8. Sensing response time versus H_2 concentration curves for various sensors prepared with different tensile strains of (a) 25%, (b) 50%, (c) 75%, and (d) 100% in response to 0.03–4% H_2 at different operating temperatures (−40 to 70 ℃).

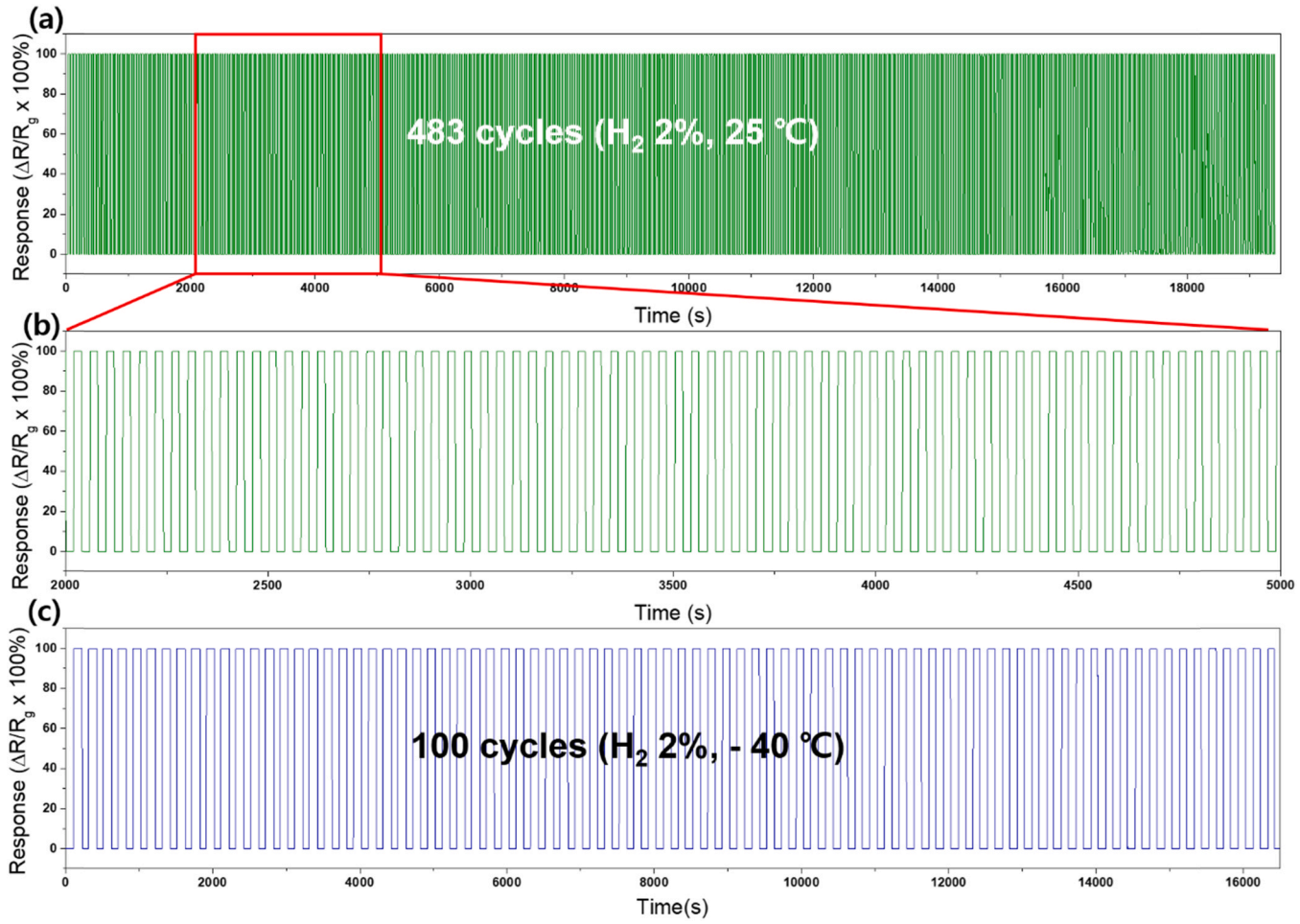

Fig. 9. Sensing reproducibility test of the Pd nanogap sensor on PDMS substrate (75% strain) exposed to 2% H_2 at different temperature environments. (a) Real-time response curves for 483 gas-in and -out cycles at 25 ℃, (b) magnified response curves measured between 2000 and 5000 s in (a), and (c) real-time response curves for 100 gas-in and -out cycles at an extremely low temperature of –40 ℃.

open gaps take part in H_2 sensing. In the case of the 120 nm width of the 50%-strained sensor, the gap width can be reduced to less than 120 nm at subzero temperatures, and thus the sensing performance can be improved compared to that at room temperature. However, the 210 nm width of the 25%-strained sensor did not affect the low-temperature sensing performance. Fig. 6 also shows that the sensing performance of the Pd nanogap sensor on PDMS is significantly reduced as the operating temperature increases above 25 ℃. With decreasing strain (increasing gap width), the current change and the maximum operating temperature decreased. For sensing 4% H_2, the maximum operating temperature was 50 ℃ for 25% strain and 70 ℃ for 100% strain. The gap width broadened, owing to the expansion of the PDMS substrate at temperatures above room temperature, as shown in Fig. 7. For example, the change in nanogap length due to the thermal effect was roughly calculated by considering the high thermal expansion coefficient (3.4×10^{-4} ℃$^{-1}$ [35]) of PDMS (Supplementary Materials). The calculation was performed on the 75%-strained sensor, which has relatively uniformly distributed nanogaps with similar inter-crack distances. The results indicated that the nanogap lengths of ~367 nm and ~306 nm can be contracted and expanded when the operating temperature is −40 ℃ and 70 ℃, respectively. In particular, the enlarged nanogap size of ~360 nm at 70 ℃ from ~52 nm at room temperature (Fig. 2(g)) can explain the degradation of the sensing performance at a high temperature of 70 ℃. Therefore, we concluded that at low and high temperatures, the sensing performances are greatly influenced by the gap width because the gap width varies according to the high thermal contraction/expansion characteristics of PDMS at those temperatures.

The sensor showing the best sensing performance at the tested temperatures from –40 to 70 ℃ for a wide range of H_2 concentrations from 4% to 300 ppm is the sensor prepared with 75% strain. In addition, the 75%-strained sensor also showed stable sensing properties after the low- and high-temperature sensing tests compared to the other sensors (Fig. S7). The response times of all sensors prepared with different strains are summarized in Fig. 8. The 25%, 50%, and 75%-strained sensors showed fast response times of less than 2 s under H_2 exposure to varying concentrations at the tested temperatures. However, the 100%-strained sensor shows a slow response time for H_2 concentrations below 0.5% at subzero temperatures. Therefore, the optimized strain value for the best sensing performance and stability in the temperature range from –40 to 70 ℃ for H_2 concentrations from 4% to 300 ppm is 75%.

Moreover, we tested the reproducibility of the 75%-strained sensor for long-term use at different temperatures of 25 ℃ and –40 ℃ by performing hundreds of sensing cycles. Fig. 9(a) shows the real-time response over 483 cycles under 2% H_2 exposure at 25 ℃. Fig. 9(b) shows the magnified response curves measured from 2000 to 5000 s in Fig. 9(a). Fig. 9(c) shows the real-time response curves for sensing 2% H_2 over 100 cycles at –40 ℃. The response of the Pd nanogap sensor on PDMS remained unchanged at 25 and –40 ℃ throughout the 483 and 100 (gas-in and -out) cycles, respectively. Therefore, the results reveal that the Pd nanogap sensor supported on PDMS showed an "On-Off" operation during hundreds of sensing cycles regardless of the environmental temperature.

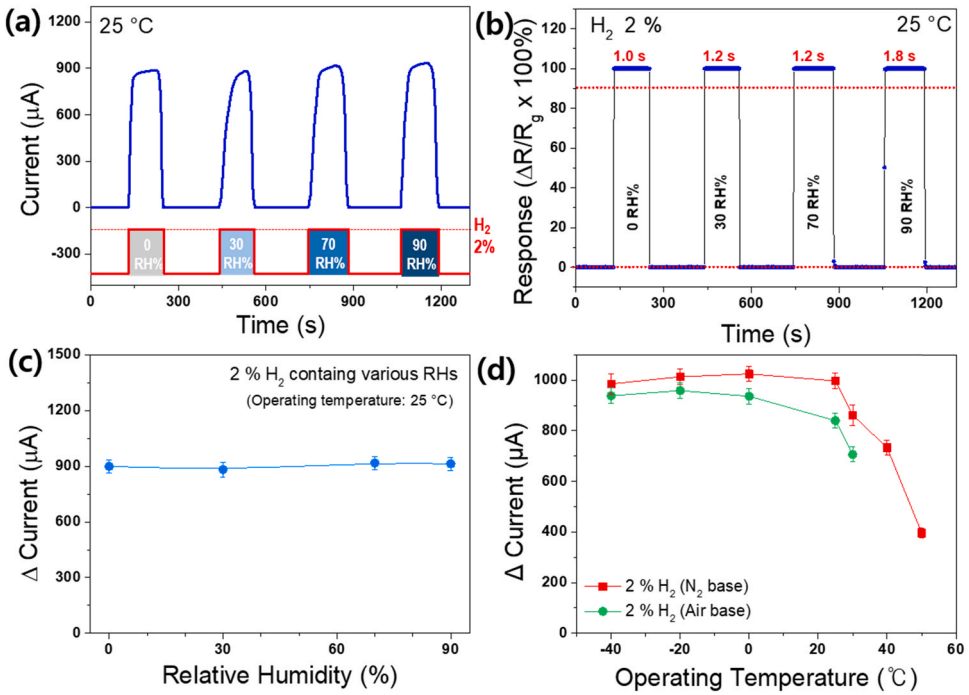

Fig. 10. (a)–(c) Humidity effect of the Pd nanogap sensor on PDMS substrate (75% strain) on the sensing performance to 2% H_2 under different humid conditions (0–90 RH%) at 25 ℃: (a) real-time current, (b) real-time response, and (c) dependence of humidity on the current change. (d) comparison of sensing properties at different operating temperatures (–40 to 50 ℃) for detecting 2% H_2 in N_2 and synthetic air.

An additional study was performed to investigate the effect of humidity on the sensing performance of the Pd nanogap sensor on the PDMS substrate at room temperature (25 °C) for practical applications. Fig. 10(a) shows the electrical responses of the 75%-strained sensor for the detection of 2% H_2 at different humidity levels (0–90 RH%) at 25 ℃. The moist H_2 gas was prepared at room temperature by mixing 2% H_2 with wet N_2, which increased the humidity level from 0 to 90 RH%. The response shows that the sensor operates in an "On-Off" mode under the different humid conditions with rapid response times within 2 s (Fig. 10 (b)). In addition, the effect of humidity on the electrical responses was analyzed by comparing the changes in the current shown in Fig. 10(c). The results reveal that the sensor is unaffected by high humidity at 25 ℃ for sensing 2% H_2.

Furthermore, the H_2-sensing properties of the sensors also need to be measured in synthetic air. However, to investigate the sensing properties of the as-prepared sensors at a relatively high H_2 concentration of 4%, N_2 was used as the balance gas owing to safety concerns. Thus, we further tested the H_2-sensing properties of the 75%-strained sensor in both N_2 and synthetic air. Fig. 10(d) shows the current variation as a function of the operating temperatures (–40 to 50 ℃) to detect 2% H_2 in a mixture of N_2 and air. The figure shows that current variations in air, compared with those in an N_2-based atmosphere, remain high at ~95% at –40 ℃ and ~82% at 30 ℃.

4. Conclusion

We investigated the effect of various environmental temperatures (–40 to 80 ℃) on the sensing performance of a Pd nanogap sensor supported on an elastomeric PDMS substrate for sensing different H_2 concentrations (0.03–4%). Through the sensing results, the utility of the Pd nanogap on the PDMS sensor as an H_2 safety sensor was verified. The sensor was prepared with different widths of the Pd nanogap by applying different tensile strains (25%, 50%, 75%, and 100%). All sensors operated in an "On-Off" mode with a rapid response time of ~1 s at temperatures ranging from –40 to 70 ℃. However, it was found that the sensing performances at low and high temperatures are greatly influenced by the gap width because the gap width varies owing to the high thermal contraction/expansion characteristics of PDMS at those temperatures. The sensing performance improved at subzero temperatures (0, –20, and –40 ℃) owing to gap narrowing, and the detection limit was as low as 300 ppm. However, at high temperatures above 40 ℃, the performance was significantly reduced, owing to the gap broadening, and the sensor could detect more than 1% H_2. Consequently, the best sensing performance, such as high current response, fast response time, and low detection limit, at all temperatures from –40 to 70 ℃ was observed in the sensor with a gap width of ~50 nm (75% strain). In addition, the 75%-strained sensor showed excellent reproducibility for hundreds of sensing cycles at 25 and –40 ℃. Furthermore, the humidity effect test showed that the sensor was stable to moisture at 25 ℃. Our study demonstrated the potential of the Pd nanogap on an elastomeric PDMS substrate for application to on-board safety H_2 sensors in hydrogen-electric vehicles by controlling the Pd gap width through the thermal contraction and expansion properties of PDMS, depending on the environmental temperature.

CRediT authorship contribution statement

Seyoung Park: Conceptualization, Investigation, Methodology, Validation. **Soo-Min Le:** Methodology, Visualization. **Jin-Kyo Jeong:** Methodology, Formal analysis, Visualization. **Donggu Kim**: Conceptualization, Validation, Visualization. **Hyunsoo Kim**: Validation, Visualization. **Hyun-Sook Lee**: Conceptualization, Validation, Writing – original draft, Writing – review & editing. **Wooyoung Lee:** Supervision.

Declaration of Competing Interest

The authors declare that they have no known competing financial interests or personal relationships that could have appeared to influence the work reported in this paper.

Acknowledgements

This research was supported by the Basic Science Research Program (2017M3A9F1052297) of National Research Foundation of Korea (NRF), the Technology Innovation Program (20013621, Center for Super Critical Material Industrial Technology) funded by the Ministry of Trade, Industry & Energy (MOTIE, South Korea), and the Priority Research Centers Program (2019R1A6A1A11055660) of NRF. H.-S. Lee thanks the Basic Research in Science and Engineering Program (2021R1A2C1013690) of NRF. Here, NRF is funded by Ministry of Science and ICT in South Korea

Appendix A. Supporting information

Supplementary data associated with this article can be found in the online version at doi:10.1016/j.snb.2021.130716.

References

[1] Reports and data, Statistics report of automotive hydrogen sensors Market. ⟨https://www.reportsanddata.com/report-detail/automotive-hydrogen-sensors-market⟩ (Accessed 17 April 2021).
[2] W. Buttner, R. Burgess, M. Post, C. Rivkin Summary and Findings from the NREL/DOE Hydrogen Sensor Workshop (June 8, 2011). 2012 Jul. Report No.: NREL/TP-5600–55645, 1048994. Available online: ⟨http://www.osti.gov/servlets/purl/1048994/⟩ (Accessed 17 April 2021).
[3] C.C. Ndaya, N. Javahiraly, A. Brioude, Recent advances in palladium nanoparticles-based hydrogen sensors for leak detection, Sensors 19 (2019) 4478.
[4] T. Hübert, L. Boon-Brett, G. Black, U. Banach, Hydrogen sensors – a review, Sens. Actuators B Chem. 157 (2011) 329–352.
[5] F. Favier, E.C. Walter, M.P. Zach, T. Benter, R.M. Penner, Hydrogen sensors and switches from electrodeposited palladium mesowire arrays, Science 293 (2001) 2227–2231.
[6] F. Yang, S.-C. Kung, M. Cheng, J.C. Hemminger, R.M. Penner, Smaller is faster and more sensitive: the effect of wire size on the detection of hydrogen by single palladium nanowires, ACS Nano 4 (2010) 5233–5244.
[7] M.A. Lim, D.H. Kim, C.-O. Park, Y.W. Lee, S.W. Han, Z. Li, R.S. Williams, I. Park, A new route toward ultrasensitive, flexible chemical sensors: metal nanotubes by wet-chemical synthesis along sacrificial nanowire templates, ACS Nano 6 (2012) 598–608.
[8] J. Kong, M.G. Chapline, H. Dai, Functionalized carbon nanotubes for molecular hydrogen sensors, Adv. Mater. 13 (2001) 1384–1386.
[9] S. Mubben, T. Zhang, B. Yoo, M.A. Deshusses, N.V. Myung, Palladium nanoparticles decorated single-walled carbon nanotube hydrogen sensor, J. Phys. Chem. C. 111 (2007) 6321–6327.
[10] J. Nah, S.B. Kumar, H. Fang, Y.-Z. Chen, E. Plis, Y.-L. Chueh, S. Krishna, J. Guo, A. Javey, Quantum size effects on the chemical sensing performance of two-dimensional semiconductors, J. Phys. Chem. C. 116 (2012) 9750–9754.
[11] I. Park, Z. Li, A.P. Pisano, R.S. Williams, Top-down fabricated silicon nanowire sensors for real-time chemical detection, Nanotechnology 21 (2010), 015501.
[12] J.-H. Ahn, J. Yun, Y.-K. Choi, I. Park, Palladium nanoparticle decorated silicon nanowire field-effect transistor with side-gates for hydrogen gas detection, Appl. Phys. Lett. 104 (2014), 013508.
[13] T.-R. Rashid, D.-T. Phan, G.-S. Chung, Effect of Ga-modified layer on flexible hydrogen sensor using ZnO nanorods decorated by Pd catalysts, Sens. Actuators B Chem. 193 (2014) 869–876.
[14] I. Sta, M. Jlassi, M. Kandyla, M. Hajji, P. Koralli, F. Krout, H. Ezzaouia, Surface functionalization of sol–gel grown NiO thin films with palladium nanoparticles for hydrogen sensing, Int. J. Hydrog. Energy 41 (2016) 3291–3298.
[15] C. Xiang, Z. She, Y. Zou, J. Cheng, H. Chu, S. Qiu, F. Xu, A room-temperature hydrogen sensor based on Pd nanoparticles doped TiO_2 nanotubes, Ceram. Int. 40 (2014) 16343–16348.
[16] B. Liu, D. Cai, Y. Liu, H. Li, C. Weng, G. Zeng, T. Wang, High-performance room-temperature hydrogen sensors based on combined effects of Pd decoration and Schottky barriers, Nanoscale 5 (2013) 2505–2510.
[17] H. Zhang, Z. Li, L. Liu, X. Xu, Z. Wang, W. Wang, C. Wang, Enhancement of hydrogen monitoring properties based on Pd–SnO_2 composite nanofibers, Sens. Actuators B Chem. 147 (2010) 111–115.
[18] M. Zhao, J.X. Huang, C.W. Ong, Diffusion-controlled H_2 sensors composed of Pd-coated highly porous WO_3 nanocluster films, Sens. Actuators B Chem. 191 (2014) 711–718.
[19] C.C. Ndaya, N. Javahiraly, A. Brioude, Recent advances in palladium nanoparticles-based hydrogen sensors for leak detection, Sensors 19 (2019) 4478.
[20] R.M. Penner, A nose for hydrogen gas: fast, sensitive H_2 sensors using electrodeposited nanomaterials, Acc. Chem. Res. 50 (2017) 1902–1910.
[21] X. Li, Y. Liu, J.C. Hemminger, R.M. Penner, Catalytically activated palladium@platinum nanowires for accelerated hydrogen gas detection, ACS Nano 9 (2015) 3215–3225.
[22] S. Cherevko, N. Kulyk, J. Fu, C.-H. Chung, Hydrogen sensing performance of electrodeposited conoidal palladium nanowire and nanotube arrays, Sens. Actuators, B 136 (2009) 388–391.
[23] K. Kyun Tae, S. Jun, C.S. Min, Hydrogen gas sensor using Pd nanowires electrodeposited into anodized alumina template, IEEE Sens. J. 6 (2006) 509–513.
[24] J. Lee, W. Shim, E. Lee, J.-S. Noh, W. Lee, Highly mobile palladium thin films on an elastomeric substrate: nanogap-based hydrogen gas, Sens., Angew. Chem. Int. Ed. 50 (2011) 5301–5305.
[25] H.-S. Lee, J. Kim, H. Moon, W. Lee, Hydrogen gas sensors using palladium nanogaps on an elastomeric substrate, Adv. Mater. (2021), 2005929.
[26] E. Lee, J. Lee, J.-S. Noh, W. Kim, T. Lee, S. Maeng, W. Lee, Pd–Ni hydrogen sponge for highly sensitive nanogap-based hydrogen sensors, Int. J. Hydrog. Energy 37 (2012) 14702–14706.
[27] T. Chang, H. Jung, B. Jang, J. Lee, J.-S. Noh, W. Lee, Nanogaps controlled by liquid nitrogen freezing and the effects on hydrogen gas sensor performance, Sens. Actuator A Phys. 192 (2013) 140–144.
[28] H. Jung, B. Jang, W. Kim, J.-S. Noh, W. Lee, Ultra-sensitive, one-time use hydrogen sensors based on sub-10 nm nanogaps on an elastomeric substrate, Sens. Actuators B Chem. 178 (2013) 689–693.
[29] B. Jang, K.Y. Lee, J.-S. Noh, W. Lee, Nanogap-based electrical hydrogen sensors fabricated fromPd-PMMA hybrid thin films, Sens. Actuators B Chem. 193 (2014) 530–535.
[30] B. Jang, S. Cho, C. Park, H. Lee, M.-J. Song, W. Lee, Palladium nanogap-based H_2 sensors on a patterned elastomericsubstrate using nanoimprint lithography, Sens. Actuators B Chem. 221 (2015) 593–598.
[31] S. Kim, B. Jang, J. Park, Y.-K. Lee, H.-S. Lee, S. Cho, W. Lee, Kinetic control of nanocrack formation in a palladium thin film on anelastomeric substrate for hydrogen gas sensing in airSungyeon, Sens. Actuators B Chem. 230 (2016) 367–373.
[32] S. Kim, H.-S. Lee, B. Jang, S. Cho, W. Lee, Strain-controlled nanocrack formation in a Pd film on polydimethylsiloxane for the detection of low H_2 concentrations, J. Mater. Sci. 51 (2016) 4530–4537.
[33] W. Kim, B. Jang, H.-S. Lee, W. Lee, Reliability and selectivity of H_2 sensors composed of Pd Film nanogaps on an elastomeric substrate, Sens. Actuators B Chem. 224 (2016) 547–551.
[34] B. Jang, W. Kim, M.-J. Song, W. Lee, Thermal stability of the sensing properties in H2 sensors composed of Pd nanogaps on an elastomeric substrate, Sens. Actuators B Chem. 240 (2017) 186–192.
[35] The Dow Chemical Company, Technical Data Sheet Sylgard 184, Form No. 11–3184–01 C, 2017. ⟨https://www.dow.com/en-us/document-viewer.html?ramdomVar=2057604309549529535&docPath=/content/dam/dcc/documents/en-us/productdatasheet/11/11–31/11–3184-sylgard-184-elastomer.pdf⟩ (Accessed 18 April 2021).
[36] M.A. Vadivelu, C. Ramesh Kumar, Girish M. Joshi, Polymer composites for thermal management: a review, Compos. Interfaces 23 (2016) 847–872.
[37] J.K. Kim, H.S. Cho, H.-S. Jung, K. Lim, K.-B. Kim, D.-G. Choi, J.-H. Jeong, K.-Y. Suh, Effect of surface tension and coefficient of thermal expansion in 30 nm scale nanoimprinting with two flexible polymer molds, Nanotechnology 23 (2012), 235303.
[38] H.C. Jamieson, G.C. Weatherly, F.D. Manchester, The α→β phase transformation in palladium–hydrogen alloys, J. Less-Common Met. 50 (1976) 85–102.
[39] S. Wagner, H. Uchida, V. Burlaka, M. Vlach, M. Vlcek, F. Lukac, J. Cizek, C. Baehtz, A. Bell, A. Pundt, Achieving coherent phase transition in palladium–hydrogen thin films, Scr. Mater. 64 (2011) 978–981.

Seyoung Park received a Bachelor's degree and a Master's degree in Materials Science and Engineering at Yonsei University in 2013 and 2021, respectively. His research interests are in various hydrogen sensors based on Pd nanogap and metal oxides.

Soo-Min Lee received a Bachelor's degree in Material Science and Engineering at Yonsei University in 2021. Since 2021, she has been studying the development of hydrogen sensing performance of Pd-based sensors as a Master's student under the guidance of Prof. Wooyoung Lee at Yonsei University.

Jin-Kyo Jeong received a Bachelor's degree in Mechanical Engineering at Inha University in 2021. Since 2021, he has been studying the development of hydrogen sensing performance of Pd-based sensors as a Master's student under the guidance of Prof. Wooyoung Lee at Yonsei University.

Donggu Kim received the B.S. and M.S. degrees from the Department of Mechanical Engineering, Inha University, Republic of Korea, in 2010 and 2012, respectively. He is currently a senior research engineer in the Institute of Fundamental & Advanced Technology Section of the Hyundai Motor Group, Korea. His research includes mid-air tactile feedback devices, and physical/chemical sensors.

Hyunsoo Kim received his Ph.D. degree in the Electrical Engineering from the Pennsylvania State University in 2010. His doctoral research involved design, modeling, and micro-fabrication of piezoelectric thin film devices. He has joined Hyundai Motor Group as a senior researcher, where his research group has focused on microelectromechanical systems (MEMS) based sensors and sensor systems for automotive applications since 2012. His current areas of interest include nanofabrication, nanoelectromechanical systems, self-powered devices, gas sensors and optical sensors.

Hyun-Sook Lee received a Ph.D. degree in Physics at POSTECH in 2008. Since 2015, she has been working as a research professor in the Department of Materials Science and Engineering at Yonsei University. Her research interests are in various materials related to high-temperature superconductors, solid-state hydrogen storages, rare-earth/rare-earth-free permanent magnets, nanostructured metal oxide semiconductor gas sensors, and Pd-based hydrogen sensors.

Wooyoung Lee is a professor of the Department of Materials Science and Engineering and the Director of Center for Super Critical Material Industrial Technology (MOTIE) at Yonsei University in Korea. He received a BS degree in Metallurgical Engineering in 1986, a MS degree in Metallurgical Engineering from the Yonsei University in 1988. He received a Ph. D. degree in Physics from University of Cambridge, United Kingdom in 2000. He is a regular member of National Academy of Engineering of Korea. He was a member of National Science & Technology Council and a director in Korea Israel Industrial R&D Foundation. In recent years, his research interests have centered on hydrogen sensors, various metal oxide semiconducting gas sensors, and breath analyzers. He is also studying thermoelectric materials and devices, and permanent magnets. He has received a number of awards in nano-related research areas and a Service Merit Medal (2008) from the Government of Korea due to contribution on the development of intellectual properties. He has authored and co-authored over 200 publications, and has edited three special books on nano-structured materials and devices.